ADVANCED FUNCTIONAL MATERIALS
www.afm-journal.de

Sunlight-Induced Cross-Linked Luminescent Films Based on Polysiloxanes and D-Limonene via Thiol–ene "Click" Chemistry

*Yujing Zuo, Jinfeng Cao, and Shengyu Feng**

The increasing pursuit of biocontained elastic materials led the investigation of the potential use of the monoterpene limonene in film synthesis via thiol–ene reaction. Poly[(mercaptopropyl)methylsiloxane] (PMMS) is first synthesized. By controlling the molar ratio of PMMS and functional monomers, such as polyethylene glycol allyl methyl ether or rhodamine-B, PMMS is partially functionalized while leaving spare mercapto groups that could be further used as cross-linking sites. On the basis of the functionalized PMMS, novel transparent silicone luminescent films with hydrophilic tunable properties are prepared by natural-sunlight-triggered thiol–ene "click" chemistry by using D-limonene as a cross-linker. Their structures and properties are thoroughly characterized. Transparent luminescent films are coated on commercially available UV-light emitting diode (LED) cell from solution medium followed by an in situ cross-linking step; a colorful LED cell is obtained through this facile and efficient method. The UV-LED coated by films show very intense photoluminescence under normal visible light or the light is on, and has very high coloric purity.

1. Introduction

Polysiloxanes have received extensive attention in the field of polymers because of their advantageous physical properties. The Si–O–Si bonds are flexible and commonly reach bond angles of 135°–180°.[1] Additionally, polysiloxanes exhibit excellent permeability and low surface energy.[2–4] Moreover, as nonpetroleum-based products, terpenes represent a cheap and abundant class of nonpolar substances with enormous potential for the synthesis of bio-based polymeric materials.[5] One of the "green" constituents, D-limonene is present in large amounts in the rind of oranges and related fruits and thus can be obtained as a by-product of the citrus industry.[6–8] This fragrant molecule has two unconjugated electron-rich alkenes with different degrees of substitution and thus is an ideal candidate for radical polymerization.[5,9] Usually, films or elastomers based on polysiloxanes are cross-linked by the following three main methods: 1) platinum-catalyzed hydrosilylation between vinyl groups and Si–H bond, 2) titanium-catalyzed condensation reaction of alkoxysilane with –OH-ended polysiloxanes, and 3) thermal-initiated free radical cross-linking reaction. However, most of these processes are catalyzed by heavy metals,[10,11] and metallic catalysts should be avoided from the standpoint of "green" chemistry.[12,13] Therefore, the establishment of a new general strategy to prepare a cross-linked polysiloxane network is imperative. The addition reaction between thiol and olefins to produce thioethers has been known for some time, and both Michael addition and free-radical addition mechanisms are depicted.[14,15] Thiol–ene "click" chemistry, a robust and environment-friendly radical-based, versatile, and rapid process in the presence of oxygen, could fulfill our anticipations.[16–19] However, most of the thiol–ene crosslink reactions are induced by UV light and can proceed at wavelengths of approximately 365 nm.[20,21] Even though thiol–ene reactions have been studied for a long time, covering different scientific fields from polymer science to biochemistry, only very few examples have been reported on thiol–ene additions irradiated by natural sunlight.[21,22] The generation of thiyl radicals using solar radiation should be possible. To the best of our knowledge, literature on cross-linking networks realized by sunlight induced thiol–ene reaction is not present to date. Thus, we focused on a novel cross-linking system synthesized under sunlight. Compared with the conventional thiol–ene reactions triggered by UV light, a sunlight-induced reaction indicates a "greener" method that does not need excessive power.

However, the typically unpleasant odors of low-molecular-weight thiols also have limited their commercial utilization.[23,24] To overcome these disadvantages and to obtain photocuring materials based on poly[(mercaptopropyl)methylsiloxane] (PMMS) with enhanced performance, we introduced D-limonene containing two different vinyl groups into PMMS to develop a novel sunlight-cured hybrid material. To take advantage of the physical and mechanical properties of polysiloxane-based materials and to allow connection with other functional molecules, PMMS was chosen as the base component for the siloxane-based systems.

Y. Zuo, J. Cao, Prof. S. Feng
Key Laboratory of Special Functional Aggregated
Materials & Key Laboratory of Colloid and Interface
Chemistry (Shandong University)
Ministry of Education
School of Chemistry and Chemical Engineering
Shandong University
Jinan 250100, P. R. China
E-mail: fsy@sdu.edu.cn

DOI: 10.1002/adfm.201500187

Additionally, the chemical modification of well-defined prepolymer chains is a valuable way to obtain functional macromolecules, and thiol–ene addition to PMMS offers tremendous versatility for molecular design.[25,26] Thus, allyl rhodamine-B and oligo(ethylene glycol) allyl methyl ether (AEM-6) were chosen to modify a PMMS side chain via thiol–ene reaction before cross-linking to obtain functional membrane films. Desired side groups are incorporated via unobtrusive thioether linkages without the introduction of additional functionalities. Moreover, by controlling the molar ratio of PMMS to functional monomers, PMMS can be partially functionalized while leaving spare thiol groups that could be further used as cross-linking sites in the preparation of PMMS-based films. After incorporation of functional groups (rhodamine-B), luminescent films were obtained, which make the composites suitable for optoelectronic devices such as light emitting diodes (LEDs). Commercial LEDs offer advantages such as environmental friendliness, low power consumption, and long lifetime.[27,28] For fast and convenient curing, the films can be obtained after coating the uncured reaction mixture onto devices of any shape. Luminescent films from the solution were coated on commercially available UV-LED cells followed by an in situ thiol–ene curing step; colorful LED cells can be fabricated through an efficient way with less cost.[29]

In this work, we report on the use of thiol–ene chemistry to photochemically cross-link a thin film based on PMMS (or functionalized PMMS) and D-limonene irradiated by sunlight, which is the first example of a "thiol–ene" sunlight-induced photocured hybrid material. In addition, the thiol–ene reaction, as a useful chemical conjugation toolbox, was adopted to synthesize functional PMMS before cross-linking to enhance the properties of the film. Moreover, cross-linked films that can be easily coated on commercially available LEDs show potential application in devices.

2. Results and Discussion

2.1. Reaction of Model Compound

Limonene represents an exceptionally versatile monomer for the introduction of new chemical functional groups that can be directed toward specific polymerization techniques.[30] Characterization of cross-linked PMMS in the molecular level is relatively difficult because of the insolubility of the network.[31,32] To obtain a deeper understanding of the reaction sites and to further the cross-linking, a small experiment using model compounds was designed. As depicted in **Scheme 1**, 1-dodecanethiol was selected as the model compound for its structural similarity with PMMS. Initially, the thiol–ene addition was performed under solvent-free conditions at room temperature. Unfortunately, this method did not work here because of insufficient miscibility of both reactants. The model reaction was carried with the least amount of THF that solubilizes D-limonene, mercaptan, and radical initiator. The ^{1}H-NMR data of 1-dodecanethiol, D-limonene, and the addition product are listed in Figure S1 (Supporting Information). Two different olefin protons of D-limonene from different positions originally located at 5.0–5.7 ppm, as well as the thiol proton of the $S{-}H$ bond of 1-dodecanethiol appearing at 1.3 ppm, disappeared. The appearance of the proton peaks around 2.5 ppm in the product is also apparent, which is attributed to the methane proton of the CH_2–S bond. These results demonstrate the efficiency of the reaction in forming the addition products based on D-limonene through a stable thioether linkage. Moreover, the quantitative reaction with a molar ratio of 1:2 of limonene and 1-dodecanethiol indicate that the two different vinyl groups could react with the thiol group. Not only have we found that the two different vinyl structures retain sufficient reactivity necessary for the thiol–ene cross-linking process, but also the existence of a slightly rigid ring that may also confer extra mechanical strength to the films.[33]

2.2. Preparation of the Cross-Linked Films

According to the conclusions obtained from the preparation of model compounds, limonene is an exceptional di-ene monomer for the preparation of thiol–ene networks. Moreover, photo-induced thiol–ene polymerizations are known to rapidly react to form highly uniform networks with narrow glass transitions and easily tailorable mechanical properties. The step-growth mechanism of polymerization favors the formation of

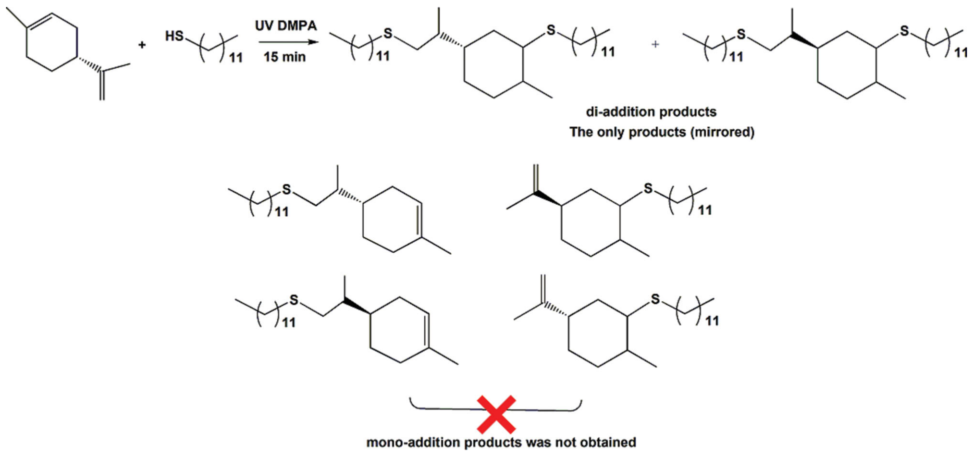

Scheme 1. Reaction route of model compounds.

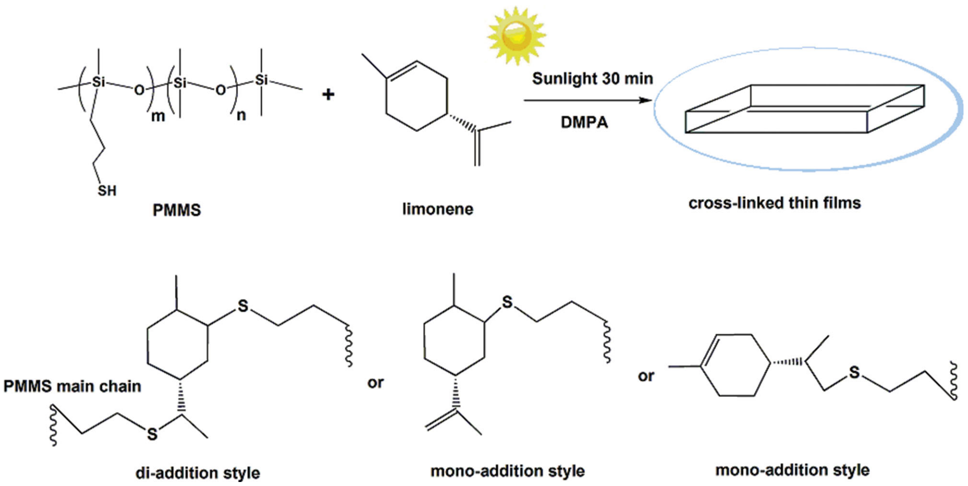

Scheme 2. Cross-linking of the silicone film networks and their different addition styles.

multiple species prior to gelation, thus resulting in high conversions at the gel point and largely homogeneous, 3D cross-linking films.[34]

For a widely used catalytic cross-linking system, the functional group tolerance, catalytic efficiency, and structural tunability are of primary concern. The DMPA (2,2–Dimethoxy–2–phenylacetophenone)-catalyzed system was selected in this study as it is expected to efficiently work with various monomers. A series of cross-linked thiol–ene networks was synthesized through photopolymerization of multifunctional PMMS with D-limonene. Before irradiation with sunlight, fixed amounts of PMMS, D-limonene, and DMPA were dissolved in THF(tetrahydrofuran) (Table S2, Supporting Information). The mixture was then poured into a Teflon mold. After curing under natural sunlight, the liquid mixture turned into a cross-linked gel, which was cut out from the mold and then immersed in dry THF several times to eliminate unreacted small molecules. As shown in **Scheme 2**, three cross-linking styles may be obtained: one represents diaddition style and the other two are monoaddition styles from two different reaction sites. The success of preparing thin films constitutes the prerequisite for a material used in device fabrication; therefore, we have prepared transparent films of the hybrid materials by drop-casting the uncross-linked reactants mixture onto flat substrates.

For preparing polysiloxane-based films, efficient cross-linking based on the design of the cross-linker and cross-linking ratio has a crucial role in building a stable polymeric network. Thiol–ene networks also require stoichiometric control to tune mechanical properties with reactive groups within the material. As listed in Table S2 (Supporting Information), a series of complexes was prepared following the same procedure with varying D-limonene content. The mechanical properties of the films were tested by identifying their Shore A hardness by using a Shore A durometer. The hardness of the resulting polymers has a direct correlation with crosslink density. Toluene swelling method was applied to measure the cross-link density (v) and M_c of the obtained films. **Table 1** shows that the number of cross-link sites obtained from a thiol–ene reaction increases from 2.63 to 4.67 with the increase in limonene content, as expected. Meanwhile, Shore A hardness increased with cross-linking density. This strategy allows for fine tuning of the mechanism properties. Moreover, other potential uses such as postfunctionalization could be further achieved either in the bulk of the material or at the film surface.

2.3. Luminescent Properties of the Films Obtained

When irradiated by UV light, cross-linked networks **C1**, **C2**, and **C3** based on PMMS emit a blue color at film state, which was derived from the coordination of the lone pair of S with Si atoms. The room temperature emission spectra of **C1**, **C2**, and **C3** excited by 330 nm are shown in **Figure 1**a. All of the films display an emission peak with a maximum wavelength (λ_{max}) of approximately 410 nm. **C1**, **C2**, and **C3** show analogic fluorescence spectra, and both the maximum emission peak and luminescent intensity were not changed when cross-linking density was altered, which also explained the absence of any effect of limonene on fluorescence properties. According to the CIE 1931 RGB colorimetric system, bright emissions of the films can be easily observed by the naked eye upon excitation with a wavelength of 330 nm, as illustrated in Figure 1b.

Unlike the carbon atom, silicon has five empty 3*d* orbitals that could be used as electron acceptors. Fluorescence was assumed to be generated by the lone pair electrons of S that coordinated with Si atoms, which is consistent with our previous report.[12] The ligand field split the 3*d* orbital of the Si atom, which was degenerated before coordination. The

Table 1. Hardness, cross-link densities and M_c of films when swollen at equilibrium.

Sample name	Swelling %	ϕ	Cross-linking density $v \times 10^4$ [mol cm^{-3}]	M_c [g mol^{-1}]	Hardness [Sh A]
C1	154	0.36	2.63	3285	26
C2	119	0.41	3.64	2498	37
C3	110	0.46	4.67	1560	44
C4	149	0.35	2.46	3350	24
C8	155	0.36	2.64	3184	23

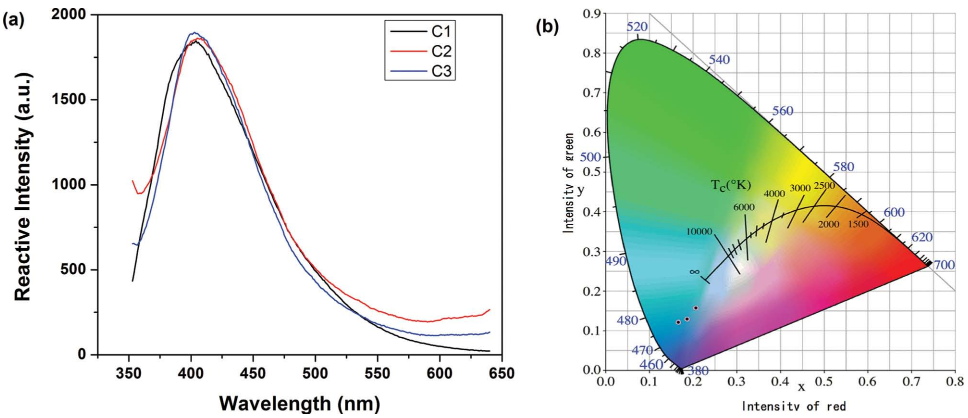

Figure 1. Fluorescence emission spectra of C1, C2, and C3 (excitation at 330 nm) a) and emission colors of films in the CIE 1931 chromaticity diagram b); CIE color coordinates: C1. (0.150, 0.131); C2. (0.183, 0.141); C3. (0.214, 0.162) *x*: intensity of red, *y*: intensity of green.

rearrangement of electrons in the split orbitals resulted in a *d–d* transition of electrons, which could be attributed to the luminescent properties of **C1**, **C2**, and **C3**.[35] As blue-light-emitting polymeric films, they promise potential implementation in future applications.

As a cheap and convenient dyestuff, rhodamine-B has excellent biocompatibility properties, high quantum yields, and large extinction coefficients.[36,37] Thus, it was chosen to modify the PMMS main chain before cross-linking to endow films with different fluorescence properties and to further expand the range of potential implementation in applications.

As shown in **Scheme 3**, transparent luminescent films were achieved after cross-linking. We directly stimulated the films at 298 K at a wavelength of 540 nm to investigate the luminescence

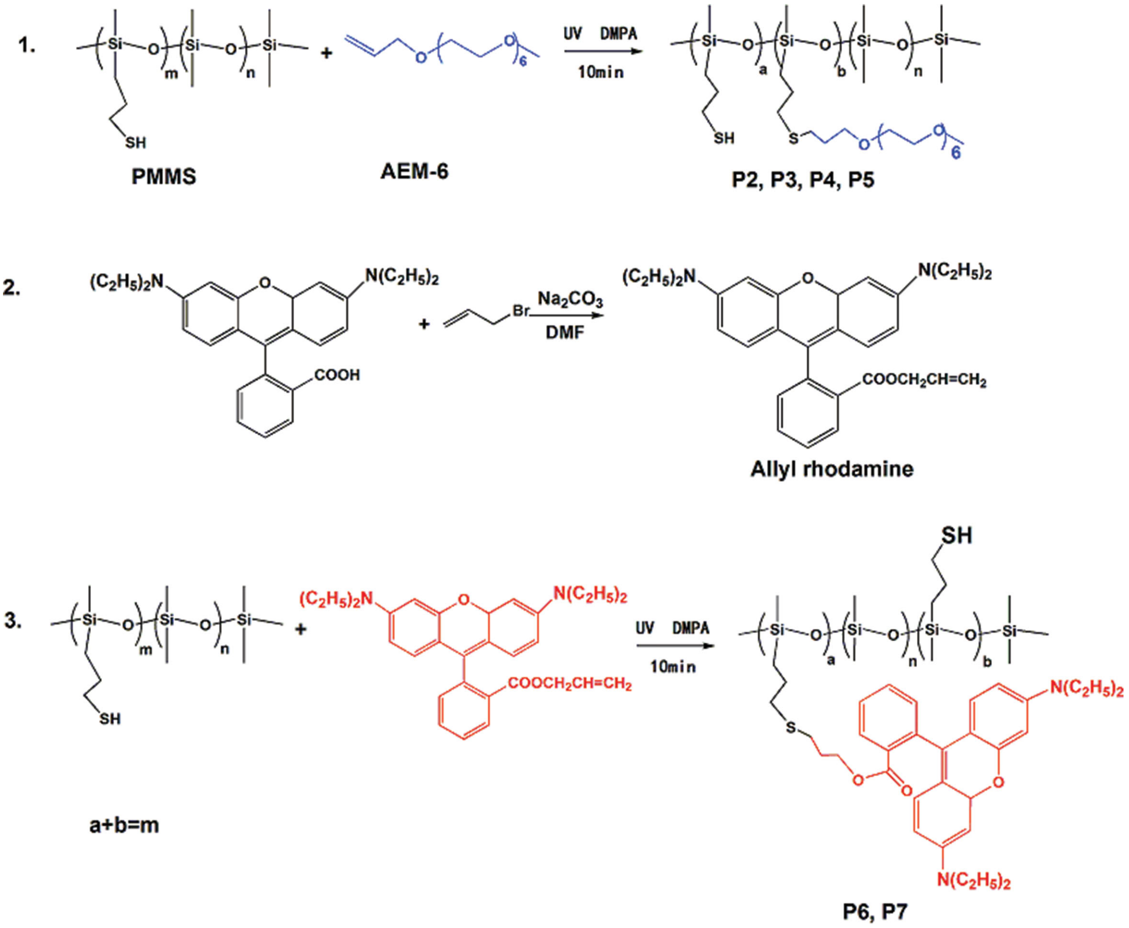

Scheme 3. Preparation of luminescent films by introducing rhodamine-B (1) and UV-LED coated with the luminescent film (2).

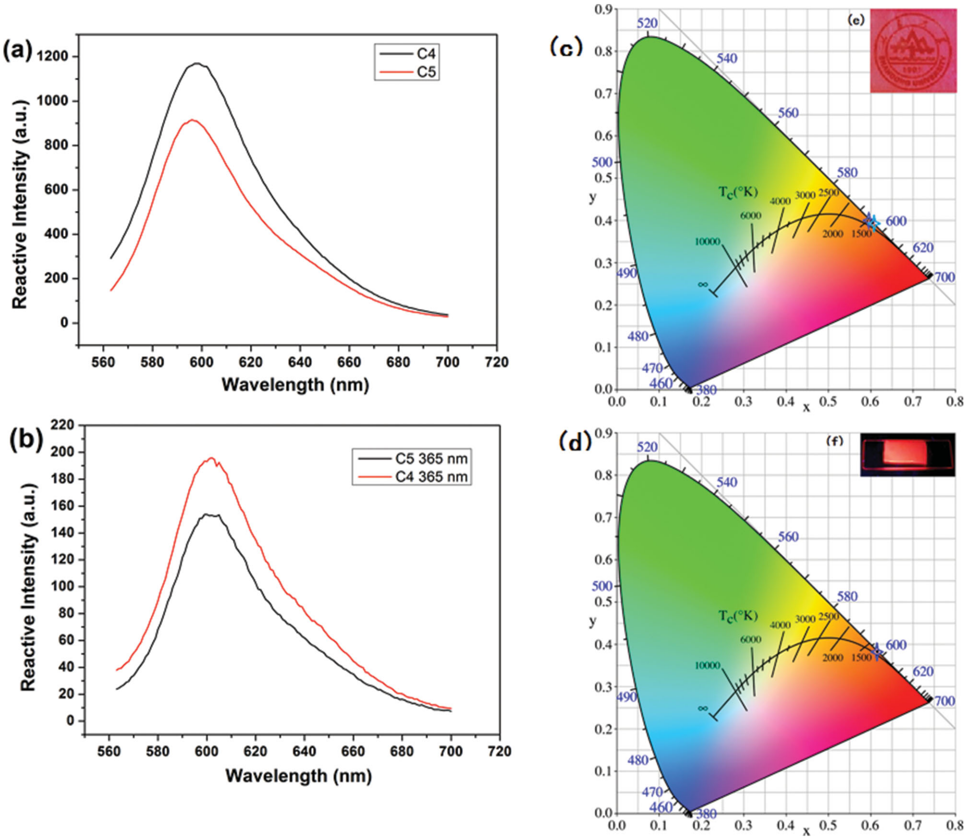

Figure 2. a) Fluorescence emission spectra of C4 and C5 (excitation at 540 nm), b) fluorescence emission spectra of C4 and C5 (excitation at 365 nm), and c) emission colors of films in the CIE 1931 chromaticity diagram; CIE color coordinates: C4. (0.601, 0.402); C5. (0.600, 0.403). d) Emission colors of films in the CIE 1931 chromaticity diagram; CIE color coordinates: C4. (0.584, 0.390); C5. (0.591, 0.383). e) Image of C4 under normal visible light. f) Image of C4 under 365 nm UV lamp illumination.

properties. The emission spectra of the luminescent film (**C4** and **C5**) are shown in **Figure 2**. The characteristic emission peak of rhodamine-B was found at a wavelength of 580 nm in **C4**. The position of the characteristic peak in **C5** did not move even after reducing the pigment content, but the intensity of the fluorescence emission decreased; thus, the novel cross-linking network does not reduce the luminescence of rhodamine by inducing "fluorescence quenching". The energy excited the fluorescence of rhodamine derived from two ways: directly excited by UV or visible light, or energy transferred from the PMMS substrate. Each dyestuff molecular was surrounded by PMMS after cross-linked step; thus, energy transferred from the PMMS substrate is the main excitation style. Using a chemical bonding style, rather than physical blending, the dispersion of rhodamine in the cross-linking system was very well, which facilitate the energy transfer between the PMMS substrate and dyestuff molecules. The intensity of fluorescence emission can be easily tuned by controlling the molar ratio of the fluorescent molecules. Human eyes are sensitive to the monochromatic spectral lights of wavelengths ca. 580 nm (red) because of the CIE1931 RGB colorimetric system. The inserted photograph of C4 (Figure 2e) shows intense red emission under normal visible light. To further explore the application of UV-LED, **C4** and **C5** were stimulated at 298 K at a wavelength of 365 nm. As shown in **Figure 3**b, the characteristic peak of rhodamine-B could also be detected at approximately 580 nm. Therefore, the bright emission of **C4** can be easily observed by the naked eye upon illumination with 365 nm excitation light provided by a 100 w ultraviolet lamp, as shown in Figure 2f. In brief,

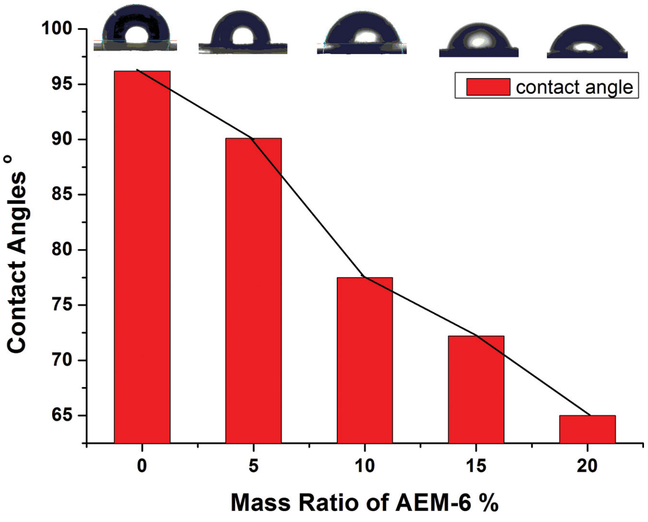

Figure 3. Contact angles of the cross-linked films: (from left to right) **C1**, **C6**, **C7**, **C8**, and **C9**.

the luminescent film prepared by sequential thiol–ene "click" chemistry shows potential applications as a coat of UV-LEDs.

2.4. Regulation of the Contact Angles

Subtle manipulation of solid surface properties is central in the design of smart materials. PDMS network was reported to have a hydrophobic surface with contact angle of 109°. Oligo(ethylene glycol) allyl methyl ether (AEM-6) was incorporated into the PMMS side chain with different molar ratios by using facile thiol–ene reaction before cross-linking. This incorporation is logical because the hydrophilic polyether segment could reduce the surface energy of the obtained cross-linked films. As shown in **Scheme 4**, a range of AEM-grafted PMMS (**P2**, **P3**, **P4**, and **P5**) was synthesized through the thiol–ene reaction of PMMS with stoichiometric AEM-6 in THF at room temperature for 10 min. The resulting products were colorless and viscous oils that were soluble in most common solvents. The resulting products were subjected to GPC and NMR measurements. In the ^{1}H NMR spectra (Figure S2, Supporting Information), the characteristic signal of the vinyl group of AEM-6 at approximately 5.5 ppm disappeared in P2, whereas the integral area of thiol peak located at 1.5 ppm diminished. Both results indicate that the thiol–ene reaction was complete. The side chain thiol protons of PMMS were originally located at 1.5 ppm, on the basis of the integral ratio of thiol peaks. The actual graft density was around 5% after thiol–ene reactions, which was a perfect match with the designed scenario. Thus, we can conclude that thiol–ene "click" chemistry is an efficient method to graft hydrophilic groups onto PMMS chains, and the graft densities can be accurately controlled by simply mixing PMMS with vinyl monomers in desired molar ratios.

Surface energies of the cross-linked thiol–ene networks were determined through static contact angle measurements. The image of the drop was calculated from the shape of the drop (both left and right contact angles) with an accuracy of ±0.1° by using an image analysis system. Distilled water was used as the test liquid. All measurements were performed at room temperature. The contact angles with different mass ratios of AEM-6 in the side chain are shown in Figure 3. The cross-linked film without AEM-6 grafted has a contact angle of 98.5°, whereas the PDMS has been reported to have a contact angle of 109°.[38] We attribute the lower contact angle to the import of the limonene that increased hydrophilicity. As expected, the contact angles decreased from 98.5° to 65.1° when AEM-6 loading was increased. The contact angles of films with AEM-6 were lower than that of the direct cross-linked network; moreover, the contact angles of the films almost linearly decreased with the increase in AEM-6 content. These results indicated that the introduction of AEM-6 could lower the contact angles of the cross-linked films, and the contact angles can further be quantitatively tuned by changing AEM-6 loading in films via chemical grafting. Inclusion of AEM side chains can render the hydrophobic PDMS a more hydrophilic surface without altering its transparency.

2.5. Thermodynamic Analysis

The thermal behavior of the cured films was evaluated by means of differential scanning calorimetry (DSC) analysis. As illustrated in Figure S3 (Supporting Information), **C1** exhibits the lowest glass transition temperature (T_g) at approximately −33 °C. The glass transition temperature of **C2** was increased to approximately −18 °C with the increase in limonene content. **C3** has the highest glass transition temperature at −4 °C, as expected. The DSC data clearly show an increase in glass transition temperature when the cross-linker content (limonene) in the photocurable formulation was increased. The increase in T_g values

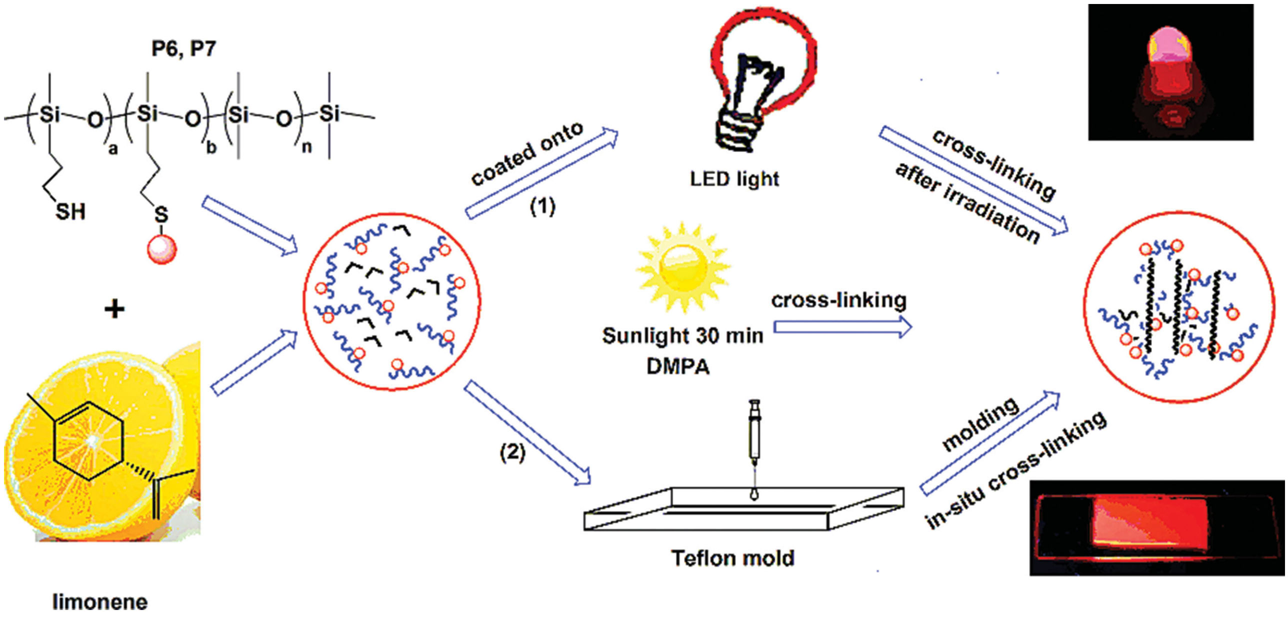

Scheme 4. Synthesis of **P2** to **P7** by thiol–ene reaction before cross-linking step.

was observed in hybrid sunlight-cured systems. This finding can be attributed to the strong interactions between the PMMS main chain and the limonene domains. The limonene imported would strongly hinder the polymeric chain mobility, reducing the segmental motion and inducing an increase in T_g values. Meanwhile, the DSC curves of the sunlight-curing films show narrow glass transition temperature range, which demonstrates that high uniformity of the formed thiol–ene networks and the photocuring is carried out by the step-growth mechanism.

Thermal gravimetric analysis (TGA) was used to investigate the effects of the different functional cross-linkers on the thermal stability of the PMMS films. The thermal stabilities of PMMS films were determined by TGA under N_2 (Figure S4, Supporting Information). PMMS films exhibited high thermal decomposition temperatures (T_d at 5 wt%) at 310 °C; thus, device fabrication by vacuum evaporation is feasible. Material decomposition occurred when temperature increased from 310 to 600 °C, and two distinct weight–loss regions were detected. Selected films initially lost weight when the temperature was from 310 to 385 °C because of organic decomposition. The mass loss rate in the second weight–loss region from 385 to 600 °C decreased as a result of the decomposition of the heat-resistant Si–C and Si–O backbones. Temperatures of initial decomposition of the different films were generally consistent, which indicate that functionalization of PMMS side chain did not affect the thermal stability of the films. C6 shows a higher amount of residue due to the introduction of poly-ether chain which has a higher carbon content.

2.6. Morphology of Cross-Linked Silicone Films

The hybrid networks obtained were highly transparent, which indicated that microphase separation in these films did not occur.[39] Morphological investigations of the dual-cured films were performed by means of scanning electronic microscopy (SEM) analysis. **C1**, **C4**, and **C8** were selected for discussion. The SEM micrographs for the cured films obtained from the mixture are shown in **Figure 4**. These images show that the phases are strictly interconnected with no macroscopic phase separation or aggregation of small molecules. The D-limonene domains are embedded in the polymeric matrix on a nanometric scale. All of them were analogous for their similar preparation procedures. As shown in Figure 4b, no change in microstructure occurred after introduction of hydrophilic groups within the membrane material (**C4**). **C8** also did not show any phase separation after the import of luminescent molecules (Figure 4c). Results indicated that this cross-linking procedure could yield a homogenous surface.[40]

2.7. Coat onto a Commercial Available UV-LED Light

The films can be easily coated on any round-shaped object because of their excellent film-forming ability, as well as their mild cross-linking reaction condition under sunlight. Instead of casting on the flat substrate to obtain the luminescent films, we coated the reactant mixture containing rhodamine-B grafted PMMS onto a commercially available UV-LED cell followed by a cross-linking step. The corresponding preparation route is illustrated in Scheme 4. As shown in **Figure 5**, a bright red light was achieved. We can conclude that the emission colors of the LED light can also be similarly tuned by changing the fluorescent molecular species or by adjusting the excitation wavelength. More types of colorful LED lights can be obtained by a similar approach.

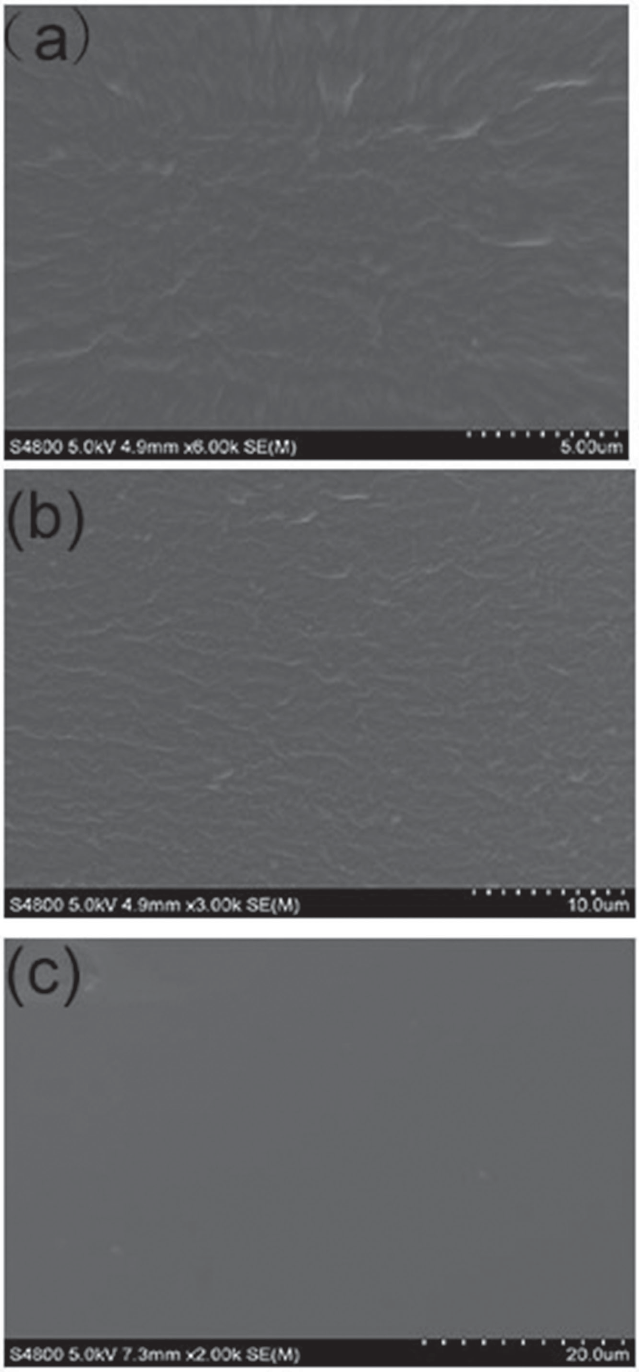

Figure 4. SEM images of cross-linked films a) **C1**, b) **C4**, and c) **C8**.

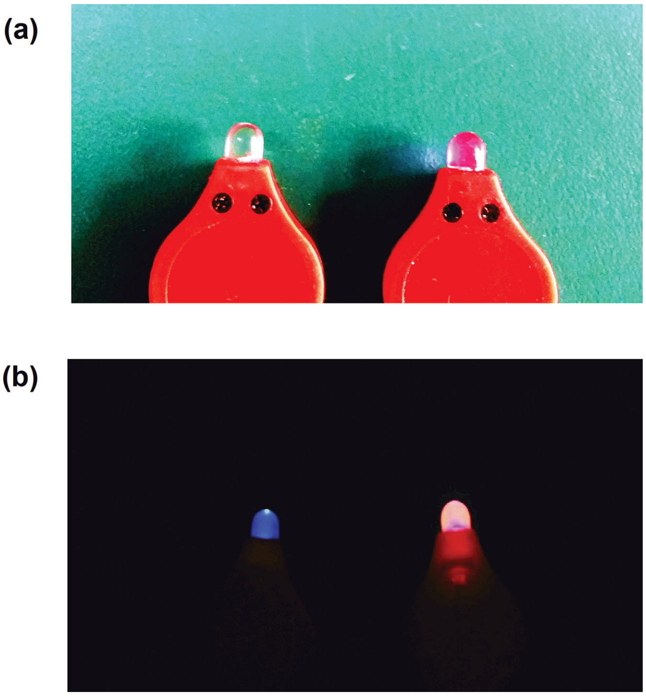

Figure 5. Images of commercial available UV-LED cell (left) and UV-LED coated with the luminescent film (right), a) under normal visible light and b) when the LED is on in a dark place.

3. Conclusion

Green hybrid films based on PMMS and D-limonene, which possess excellent film properties, were developed. Such a robust material offers tunability of mechanical and chemical properties under simplified processing conditions, which further decreases the barrier to exploiting polysiloxane-based films while increasing the range of possible applications. These transparent films could be coated on round-shaped objects, such as UV-LED cell from solution medium, before cross-linking, which makes them ideal candidates for fabricating devices used as display and lighting in an environment-friendly way. Most importantly, this study demonstrates how an appropriate synthesis strategy can be applied to terpene monomers while allowing the development of new environmentally benign materials.

4. Experimental Section

Materials: 2,2–Dimethoxy–2–phenylacetophenone (DMPA) and D-limonene were purchased from Aladdin Co. (China) and used as received. Oligo(ethylene glycol) allyl methyl ether (AEM-6), 3-Mercaptopropylmethyldimethoxysilane (MPDMS) and Dimethoxydimethylsilane were purchased from Diamond Advanced Material of Chemical Inc. (China) and distilled before use. Tetrahydrofuran (THF) was purified according to routine procedure and distilled over sodium before use.

Characterization and Measurements: Proton nuclear magnetic resonance (^{1}H NMR) spectra were recorded on a Bruker AVANCE 400 spectrometer at 25 °C using $CDCl_3$ as solvent and without tetramethylsilane as an interior label. Gel permeation chromatography measurements were carried out in THF (1 mL min^{-1}) at 40 °C with a Waters 515 liquid chromatograph (Milford, MA) equipped with a refractive-index detector 2414. DSC measurements were studied using SDTQ 600 of TA Instruments. The films were loaded in aluminum pans, heated from 25 to 200 °C. The heating and cooling temperature ramping rates were 10 °C min^{-1}. Thermogravimetric analysis (TGA) was performed under N_2 using a TA SDTQ600 at a temperature range of room temperature to 800 °C with a heating rate of 10 °C min^{-1}. Contact angle was detected using a Data physics OCA–20 contact angle analyzer with distilled water as the test liquid. Scanning electronic microscopy (SEM) images were obtained using Hitachi S–4800 (7 kV). The samples were cut and coated with a thin layer of gold before the investigation. The luminescence (excitation and emission) spectra of the samples were determined with a Hitachi F–4500 fluorescence spectrophotometer using a monochromated Xe lamp as an excitation source. Excitation and emission slits measured 5 and 2.5 nm, respectively. Hardness (Shore A) of films were measured according to ASTMD 2240–2005 method using a Shore durometer (Laizhou Huayin Research Instruments Co., China).

Synthesis of PMMS: PMMS was synthesized according to the classical procedure.[11] Yield: 80%. ^{1}H-NMR (400 MHz, $CDCl_3$): $\delta = 0.01$–0.25 (m, $-\mathrm{Si}\mathit{CH}_3$), 0.60–0.75 (m,$-\mathrm{Si}\mathit{CH}_2\mathrm{CH_2CH_2SH}$), 1.31 (s, $-\mathit{SH}$), 1.60–1.75 (m, $-\mathrm{SiCH_2}\mathit{CH}_2\mathrm{CH_2}\mathit{S}-$), 2.55–2.60 (m, $-\mathrm{SiCH_2CH_2}\mathit{CH}_2\mathrm{SH}$). The gel permeation chromatography (GPC) data of PMMS was listed in Table S1 (Supporting Information).

Synthesis of Allyl Rhodamine B: Allyl rhodamine B was synthesized according to the classical procedure.[41] ^{1}H-NMR(400 MHz, $CDCl_3$): 1.31 (t, 12H), 3.69 (q, 8H), 4.46 (d, 2H), 5.05–5.12 (m, 2H), 5.59–5.66 (m, 1H), 7.00 (d, 2H), 7.05 (dd, 2H), 7.11 (d, 2H), 7.46 (d, 1H), 7.82 (t, 1H), 7.89 (t, 1H), 8.32 (d, 1H).

Synthesis of Functionalized PMMS (P2–P7): The structures and synthetic route of functionalized PMMS are shown in Scheme 3. A series of complexes (Table S2, Supporting Information) was prepared following the same procedure. AEM–functionalized polysiloxane (**P2**) was synthesized by a literature procedure.[21] 0.10 g (0.29 mmol) AEM-6, 2.00 g PMMS, and 0.04 g (0.15 mmol) DMPA were dissolved in glass vessels containing a mixed solvent of dry THF. The vessels were placed under UV-light irradiation (365 nm, 100 w) and stirred gently for 10 min at room temperature. The resulting product was purified by H_2O precipitation, followed by vacuum drying at 50 °C for 24 h. Yield: 99%. ^{1}H NMR (400 MHz, $CDCl_3$, ppm): $\delta = 0.01$ to 0.25 (m, $-\mathrm{Si}\mathit{CH}_3$), 0.60–0.75 (m,$-\mathrm{Si}\mathit{CH}_2\mathrm{CH_2CH_2}\mathit{S}-$), 1.31 (s, $-\mathit{SH}$), 1.60–1.75 (m, $-\mathrm{SiCH_2}\mathit{CH}_2\mathrm{CH_2}\mathit{S}-$), 1.75–1.80 (m, $-\mathrm{SiCH_2}\mathit{CH}_2\mathrm{CH_2SCH_2}-$), 2.55–2.60 (m, $-\mathrm{SiCH_2CH_2}\mathit{CH}_2\mathrm{SH}$), 2.65–2.70 (m, $-\mathrm{SiCH_2CH_2}\mathit{CH}_2\mathrm{S}\mathit{CH}_2-$), 3.37(s, $\mathrm{O}\mathit{CH}_3$), 3.52 (m, $-\mathrm{O}\mathit{CH}_2-$). Rhodamine B-functionalized polysiloxane (**P6** or **P7**) was obtained by a similar procedure. Yield: P6: 95%, P7: 93%. ^{1}H NMR (400 MHz, $CDCl_3$, ppm): $\delta = 0.01$–0.25 (m, $-\mathrm{Si}\mathit{CH}_3$), 0.60–0.75 (m,$-\mathrm{Si}\mathit{CH}_2\mathrm{CH_2CH_2S}$), 1.31 (s, $-\mathit{SH}$), 2.55–2.60 (m, $-\mathrm{SiCH_2CH_2}\mathit{CH}_2\mathrm{S}$), 3.67–3.73 (q), 4.43–4.46 (d), 7.00–8.32 (m, Ar–H) The GPC data of P2–P7 are listed in Table S1 (Supporting Information).

Preparation of Silicone Films (C1–C9) by Sunlight-Induced Thiol–ene Reaction: The methods of film preparation films are shown in Schemes 2, 3. A series of complexes (see Table S2, Supporting Information) was prepared following the same procedure. Taking C1 as an example, cross-linking was achieved by mixing PMMS and the bifunctional cross-linker D-limonene. PMMS was dissolved in THF. D-limonene and DMPA were gradually added to the mixtures. The mixture was poured into a Teflon mold, and the solvent was evaporated. The mold was cured under sunlight to obtain a transparent silicone film (**C1**). Finally, the obtained film was submerged in THF for 72 h. THF was changed every 24 h to ensure that all uncross-linked materials and photoinitiator residues were removed from the network.

Measurement of Cross-Linking Density: Extent of crosslinking of the samples was measured by swelling at equilibrium. The samples were immersed in toluene solvent for 72 h. The equilibrium toluene content in the sample was determined using Equation (1)

$$\%\mathrm{swelling} = \left(\frac{w_t - w_0}{w_0}\right) \times 100 \quad (1)$$

Cross-link density of the samples was calculated by the Flory and French Equation (2)

$$\nu_e = \frac{\rho}{M_c} = \frac{-\left[1n(1-\varphi)+\varphi+\chi\varphi^Z\right]}{V_0\varphi^{\frac{1}{3}}} \tag{2}$$

where M_c is the average molecular weight between two cross-linking points, ν_e is the cross-link density of the sample, φ is the volume fraction of the rubber in the swollen sample, χ is the rubber solvent interaction parameter, ρ is the density of the rubber before swelling, and V_0 is the molar volume of the solvent.

Supporting Information

Supporting Information is available from the Wiley Online Library or from the author.

Acknowledgements

This work was financially supported by the National Natural Science Foundation of China (Grant Nos. 21274080 and 21204043) and Special Fund for Shandong Independent Innovation and Achievements transformation(Grant No. 2014ZZCX01101.

Received: January 16, 2015
Revised: March 5, 2015

---

[1] Y. Zuo, H. Lu, L. Xue, X. Wang, L. Ning, S. Feng, *J. Mater. Chem. C* **2014**, *2*, 2724.
[2] Y. Meng, Z. Wei, L. Liu, L. Liu, L. Zhang, T. Nishi, K. Ito, *Polymer* **2013**, *54*, 3055.
[3] D. Zhuo, A. Gu, G. Liang, J.-t. Hu, L. Yuan, X. Chen, *J. Mater. Chem.* **2011**, *21*, 6584.
[4] D. Sun, Q. Fu, Z. Ren, W. Li, H. Li, D. Ma, S. Yan, *J. Mater. Chem. C* **2013**, *1*, 5344.
[5] R. Ciriminna, M. Lomeli-Rodriguez, P. D. Carà, J. A. Lopez-Sanchez, M. Pagliaro, *Chem. Commun.* **2014**, *50*, 15288.
[6] M. Pourbafrani, G. Forgács, I. S. Horváth, C. Niklasson, M. J. Taherzadeh, *Bioresource Technol.* **2010**, *101*, 4246.
[7] W. Duetz, H. Bouwmeester, J. Van Beilen, B. Witholt, *Appl. Microbiol. Biotechnol.* **2003**, *61*, 269.
[8] R. Mülhaupt, *Macromol. Chem. Phys.* **2013**, *214*, 159.
[9] L. A. Pfaltzgraff, E. C. Cooper, V. Budarin, J. H. Clark, *Green Chem.* **2013**, *15*, 307.
[10] F. Gonzaga, G. Yu, M. A. Brook, *Macromolecules* **2009**, *42*, 9220.
[11] L. Xue, Y. Zhang, Y. Zuo, S. Diao, J. Zhang, S. Feng, *Mater. Lett.* **2013**, *106*, 425.
[12] Y. Zuo, D. Wang, J. Zhang, S. Feng, *RSC Adv.* **2014**, *4*, 62827.
[13] A. K. Tucker-Schwartz, R. A. Farrell, R. L. Garrell, *J. Am. Chem. Soc.* **2011**, *133*, 11026.
[14] C. E. Hoyle, C. N. Bowman, *Angew. Chem. Int. Ed.* **2010**, *49*, 1540.
[15] A. Dondoni, *Angew. Chem. Int. Ed.* **2008**, *47*, 8995.
[16] H. C. Kolb, M. Finn, K. B. Sharpless, *Angew. Chem. Int. Ed.* **2001**, *40*, 2004.
[17] H. Lu, J. A. Carioscia, J. W. Stansbury, C. N. Bowman, *Dental Mater.* **2005**, *21*, 1129.
[18] N. B. Cramer, T. Davies, A. K. O'Brien, C. N. Bowman, *Macromolecules* **2003**, *36*, 4631.
[19] C. Kuttner, P. C. Maier, C. Kunert, H. Schlaad, A. Fery, *Langmuir* **2013**, *29*, 16119.
[20] M. J. Kade, D. J. Burke, C. J. Hawker, *J. Polym. Sci., Part A: Polym. Chem.* **2010**, *48*, 743.
[21] N. B. Cramer, S. K. Reddy, M. Cole, C. Hoyle, C. N. Bowman, *J. Polym. Sci., Part A: Polym. Chem.* **2004**, *42*, 5817.
[22] N. Ten Brummelhuis, C. Diehl, H. Schlaad, *Macromolecules* **2008**, *41*, 9946.
[23] L. M. Campos, I. Meinel, R. G. Guino, M. Schierhorn, N. Gupta, G. D. Stucky, C. J. Hawker, *Adv. Mater.* **2008**, *20*, 3728.
[24] G. Franc, A. K. Kakkar, *Chem. Soc. Rev.* **2010**, *39*, 1536.
[25] A. J. Magenau, J. W. Chan, C. E. Hoyle, R. F. Storey, *Polym. Chem.* **2010**, *1*, 831.
[26] Y. Lv, Y. Cao, F. Svec, T. Tan, *Chem. Commun.* **2014**, *50*, 13809.
[27] T. Nishida, H. Saito, N. Kobayashi, *Appl. Phys. Lett.* **2001**, *79*, 711.
[28] K. H. Kwon, W. B. Im, H. S. Jang, H. S. Yoo, D. Y. Jeon, *Inorg. Chem.* **2009**, *48*, 11525.
[29] T. Wang, P. Li, H. Li, *ACS Appl. Mater. Interfaces* **2014**, *6*, 12915.
[30] M. Claudino, J.-M. Mathevet, M. Jonsson, M. Johansson, *Polym. Chem.* **2014**, *5*, 3245.
[31] U. Müller, A. Kunze, C. Herzig, J. Weis, *J. Macromol. Sci., Part A: Pure Appl. Chem.* **1996**, *33*, 439.
[32] R. F. Teixeira, O. van den Berg, L.-T. T. Nguyen, K. Fehér, F. E. Du Prez, *Macromolecules* **2014**, *47*, 8231.
[33] M. Claudino, M. Jonsson, M. Johansson, *RSC Adv.* **2014**, *4*, 10317.
[34] R. Pötzsch, B. C. Stahl, H. Komber, C. J. Hawker, B. I. Voit, *Polym. Chem.* **2014**, *5*, 2911.
[35] M. Fujiki, J. R. Koe, K. Terao, T. Sato, A. Teramoto, J. Watanabe, *Polym. J.* **2003**, *35*, 297.
[36] M. Nakamura, K. Ishimura, *Langmuir* **2008**, *24*, 5099.
[37] V. Tsyalkovsky, V. Klep, K. Ramaratnam, R. Lupitskyy, S. Minko, I. Luzinov, *Chem. Mater.* **2007**, *20*, 317.
[38] J. T. Han, D. H. Lee, C. Y. Ryu, K. Cho, *J. Am. Chem. Soc.* **2004**, *126*, 4796.
[39] L. Li, R. Liang, Y. Li, H. Liu, S. Feng, *J. Colloid Interface Sci.* **2013**, *406*, 30.
[40] J. Han, H. Lu, J. Zhang, S. Feng, *Mater. Chem. Phys.* **2012**, *136*, 36.
[41] Q.-H. Liu, J. Liu, J.-C. Guo, X.-L. Yan, D.-H. Wang, L. Chen, F.-Y. Yan, L.-G. Chen, *J. Mater. Chem.* **2009**, *19*, 2018.